Rotator cuff regeneration using chitin fabric as an acellular matrix

Tadanao Funakoshi, MD, PhD,[a,b] Tokifumi Majima, MD, PhD,[a,b] Naoki Suenaga, MD, PhD,[a] Norimasa Iwasaki, MD, PhD,[a,b] Shintaro Yamane, MD, PhD,[a,b] and Akio Minami, MD, PhD,[a,b] *Sapporo, Japan*

Twenty-one rabbits were used to investigate the feasibility of using nonwoven chitin fabric as an acellular matrix for rotator cuff regeneration. Infraspinatus tendons were cut bilaterally to create 10 × 10–mm defects. The defect in the right shoulder was covered with chitin fabric. The contralateral defect was left free as a control. The specimens were evaluated histologically and immunohistochemically at 2, 4, 8, and 12 weeks and biomechanically at 12 weeks after surgery. The acellular matrix increased cell numbers and improved collagen fiber alignment. The regenerated tissues were composed of type III collagen. The structural properties of the grafted shoulder were significantly greater than those of the control. This study revealed that using chitin fabric as an acellular matrix has advantages in enhancing both biologic and mechanical regeneration of rotator cuff tendons. (J Shoulder Elbow Surg 2006; 15:112-118.)

Rotator cuff tears can cause intolerable chronic pain and severe functional disability. Although rotator cuff tears have been treated with nonsurgical therapy, massive tears occasionally necessitate surgical reconstructive procedures, including tendon transfers or patch plasties.[6,9,20] However, there are limitations with the present surgical procedures. Tendon transfer has donor site morbidity, and polytetrafluoroethylene felt grafts cause wear particle arthritis. Regarding novel approaches to rotator cuff treatment, Dejardin et al[3] reported that porcine small intestine submucosa was an effective material for maintaining the mechanical strength of the reconstructed rotator cuff and Thomopoulus et al,[24] showed that fibrin clots enhanced the healing of a rat supraspinatus tendon defect. Although these studies have shown the feasibility of using biodegradable materials for regeneration of rotator cuff tendons, a number of limitations to the clinical application of these engineering techniques remain, including immunologic reactions and the inadequate mechanical strength of these materials.

Tissue engineering is an emerging scientific approach that attempts to develop biologic substitutes made from isolated cells and 3-dimensional polymeric scaffolds.[11] Although, in tissue engineering, the result should include functional cells, there are strategies to recruit cells from the recipient or host by use of non–cell-seeded implants. Nerem[17] has advanced an approach using an acellular biodegradable matrix organized with 3-dimensional architecture mimicking a specific tissue. Because the infiltrating cells are the patient's own cells, there is no need for any engineering to achieve immune acceptance. This approach, which can enhance tissue regeneration, has the potential to overcome the limitations of current reconstructive procedures. In this method, a biodegradable matrix acts as a temporary template until native extracellular matrices have matured through the process of tissue regeneration. Furthermore, the matrix should be a biologic stimulator to recruit cells and regulate cell adhesion, proliferation, differentiation, and matrix remodeling.[8]

Chitin is a biocompatible and biodegradable material with low immunogenicity that does not induce toxic reactions in living bodies. In addition, it has been reported that chitin enhances cellular proliferation and migration.[23] On the basis of these favorable biologic effects, chitin has been used as an ideal biopolymer with a wide variety of biomedical and industrial applications.[14] In particular, several studies have reported that chitin accelerated wound healing[7,16,23,25] and that chitin derivatives enhanced regeneration of skin tissue.[15] We hypothesized that the biologic effects of chitin could be beneficial for the regeneration of the rotator cuff tendon, as well as of epidermal tissues. With regard to the mechanical strength of chitin fabric, we can easily control the strength by altering the pore size and the thickness of the fabric. These facts suggest that chitin would be an

From the Department of Orthopaedic Surgery, Hokkaido University School of Medicine, and Frontier Research Center for Postgenomic Science and Technology, Hokkaido University.

Reprint requests: Tadanao Funakoshi, MD, Department of Orthopaedic Surgery, Hokkaido University School of Medicine, Kita 15 Nishi 7 Kita-ku, Sapporo 060-8638, Japan. (E-mail:t-funa@med.hokudai.ac.jp).

1058-2746/2006/$32.00

doi:10.1016/j.jse.2005.05.012

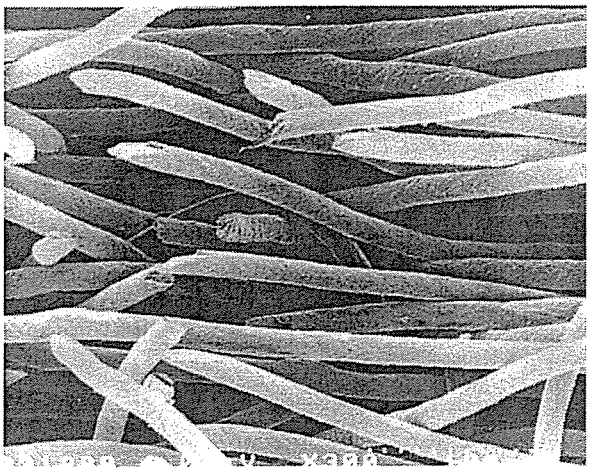

Figure 1 Scanning electron micrograph of nonwoven chitin fabric (original magnification ×3000).

advantageous material as an acellular matrix for the treatment of rotator cuff tendon defects.

The objective of this study was to investigate histologically and biomechanically the feasibility of using nonwoven chitin fabric as an acellular matrix for the regeneration of rotator cuff tendon defects.

MATERIALS AND METHODS

Nonwoven chitin fabric, an improvement from Beschitin W-A (Unitica, Kyoto, Japan), was used in this study (Figure 1). The mechanical properties of the chitin fabric were measured by use of the Japanese Industrial Standards L1015 under dry and wet conditions. Mechanical tests were performed on 5 samples at a crosshead speed of 20 mm/min by use of a material testing machine (P/N346-51299-02; Shimadzu, Kyoto, Japan). Each side of the fabric was nipped with a strip of a paper and mounted on the upper and lower chucks. We confirmed that there was no slippage of the clamps' grip.

Animal experimentation was carried out in the Institute of Animal Experimentation, Hokkaido University School of Medicine, Hokkaido, Japan, under the Rules and Regulations of the Animal Care and Use Committee, Hokkaido University School of Medicine. Twenty-one mature Japanese white rabbits, weighing 3 kg, were used in this study. Under general anesthesia induced by use of intravenous pentobarbital injection (0.05 mg/kg body weight), followed by anesthesia with isoflurane in oxygen, both infraspinatus tendons including the humeral insertion were removed to create a defect of 10 mm in length and 10 mm in width (Figure 2,*A*). A trough was created in the cortical bone over the insertion of the infraspinatus tendon until cancellous bone was exposed. In the right shoulder, the defect was covered with a 10 × 10–mm patch of nonwoven chitin fabric (grafted shoulder group) (Figure 2,*B*). The distal end of the fabric was fixed into the bony trough with two 3-0 nylon mattress sutures, and the proximal stump of the fabric was sutured to the infraspinatus tendon via the same technique. The 4 corners of the chitin fabric in the right shoulder and the corner of the defect in the left shoulder were sutured in a way to show defined markers. The defect of the contralateral (left) shoulder was left free as a control (control shoulder group). After surgery, the animals were not immobilized and were allowed to move freely in their cages.

Four rabbits were sacrificed for histologic and immunohistochemical analyses at each of 4 stages (2, 4, 8, and 12 weeks) by use of an intravenous overdose of pentobarbital. En bloc specimens including the greater tuberosity were harvested from each shoulder. The specimens were fixed in 10% buffered formalin and decalcified in formaldehyde and formic acid. Specimens were split to obtain longitudinal sections from the grafted and control shoulders. The sections were embedded in paraffin wax and cut into 5-μm-thick longitudinal sections, which were then stained with hematoxylin-eosin and safranin O. For the immunohistochemical analysis, mouse monoclonal antibodies to human collagen type I, type II, and type III (1:100) (Fujichemicals, Takaoka, Japan) were used.[10] The sections were washed 3 times and incubated with the peroxidase-labeled polymer-conjugated antirabbit antibody (Envision system, DakoCytomation, California Inc, Carpinteria, CA) for 1 hour. Antibody binding was visualized by use of 3,3'-diaminobenzidine tetrahydrochloride.

At 4 weeks after surgery, both shoulders of 5 rabbits were obtained for biomechanical evaluation. The rotator cuff tendon-humerus complex was dissected free, and the surrounding tissues were carefully removed with reference to the 4 corner suture markers. The cross-sectional area of each specimen was measured by use of the contact method with an area micrometer (2050F-60, Mitutoyo, Tokyo, Japan), as reported previously.[12,13] A bone-tendon preparation was mounted and attached to a conventional tensile tester (P/N346-51299-02, Shimadzu). The tendons of both groups were cut to create a dumbbell shape, 3 mm in width, for biomechanical study. The free end of the tendon was secured with a specially designed cryo-jaw device.[21] The mechanical testing outlined previously was performed.[12,13] After a preload of 0.5 N was applied for 10 minutes, the specimen was subjected to 10 cycles of loading and unloading for preconditioning between 0 and 0.5 mm of crosshead displacement. Mechanical tests were performed at a crosshead speed of 20 mm/min. A load-deformation curve was obtained from the load-displacement relationship. The stiffness was defined by the slope after the toe region, by use of least squares linear regression analysis.

Statistical comparisons were performed by use of the Student *t* test. $P < .05$ was considered to be statistically significant.

RESULTS

Mechanical properties of acellular matrix

In dry conditions, the mean failure load and elongation at failure of the nonwoven chitin fabric (10 mm in width, 15 mm in length, and 4 mm in thickness) were 9.4 ± 1.2 N (mean ± SD) and 19.4% ± 5.4%, respectively. After 4 weeks of incubation in Dulbecco's modified Eagle's medium (D5796, Sigma Chem-

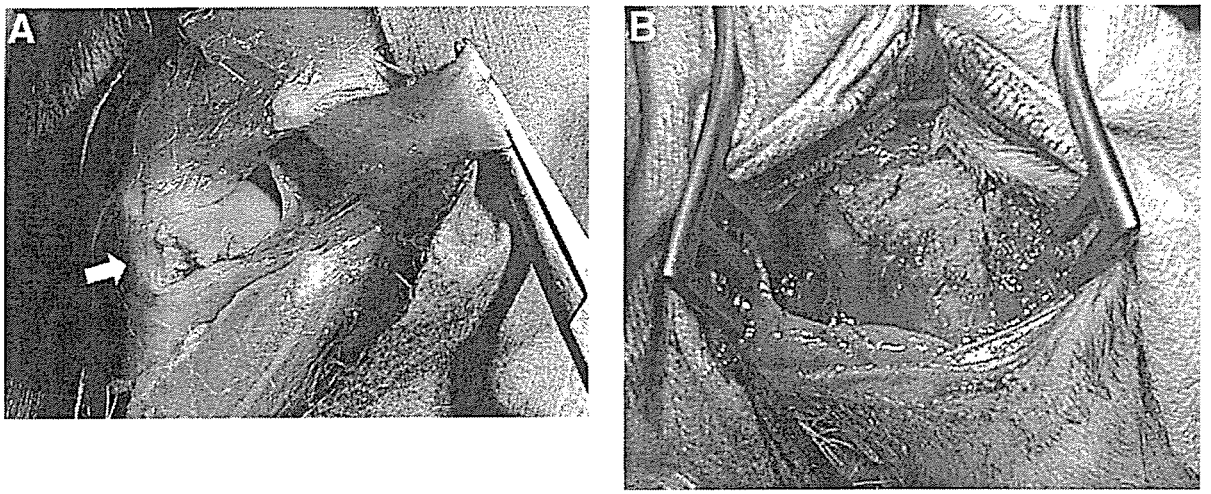

Figure 2 Surgical procedure. **A**, Infraspinatus tendons from a rabbit were removed bilaterally to create the defects. A bony trough was created over the insertion of the infraspinatus (*arrow*). **B**, Nonwoven chitin fabric was inserted into the defect.

ical Co, St Louis, MO) with 10% fetal bovine serum (10099-141; Invitrogen Corp, Carlsbad, CA), the mean failure load and elongation at failure of the nonwoven chitin fabric were 11.23 ± 0.92 N and 40.9% ± 2.5%, respectively. There were no significant differences in the failure load between dry and wet conditions. On the other hand, the elongation at failure after 4 weeks of incubation significantly increased compared with dry conditions.

Gross observation

Macroscopically, all created defects in the grafted shoulder group were covered with thick regenerated tissue between the rotator cuff and humerus at each time point. In the control shoulder group, at 2 and 4 weeks, the regenerated tissue could not be divided from the deltoid muscle, whereas at 8 and 12 weeks, the defects were covered with fibrous tissue. There were no macroscopic findings, including severe edema or discharge, indicating significant immune reactions around the grafted chitin fabric in all shoulders at all times.

Histologic evaluation

At 2 weeks, in the grafted shoulder group, a small number of fibroblasts were observed on the layer of the fabric by the side of the deltoid muscle and tendon-bone insertion (Figure 3, *A*). Collagen fibers were not clearly detected. The chitin fibers had not been absorbed. On the other hand, in the control shoulder group, the firm membrane was absent and only blood cells and fibrin clots were observed at the tendon defect site (Figure 3, *B*). At 4 weeks, in the grafted shoulder group, the regenerated tissue and the number of fibroblasts were significantly increased compared with at 2 weeks. Collagen fibers were obvious along the direction of the longitudinal tendon (Figure 4, *A*). The crimp pattern of the tendon was partially evident. Although the chitin fibers stayed in their original form, a small amount of collagen fiber was observed inside the fabric substance. In the control shoulder group, there was a thin membrane with a large number of fibroblasts and vessels (Figure 4, *B*). At 8 weeks, the same measures in the grafted shoulder group were similar to those at 4 weeks, and a small amount of the chitin material had been absorbed (Figure 5). From 8 to 12 weeks, the regenerated tissue gradually thickened in the grafted shoulder group; the fabric was absorbed and changed to an irregular form (Figure 6, *A*). With the absorption of the fabric, the number of fibroblasts decreased. The regenerated tissue in the grafted shoulder group was thicker than that in the control group (Figure 6, *B*). The collagen fibers and their characteristic crimp patterns were oriented regularly. At all time points, all specimens showed minimal evidence of monocytic infiltration or inflammatory response around the chitin fabric. Angiogenesis was not obviously apparent in either experimental group. At the tendon-to-bone insertion, the direction of the collagen fibers was not perpendicular to the bone in the grafted shoulder group at 2 weeks (Figure 3, *A*). The perpendicular pattern of collagen fibers inserted in the bone was observed in one of the grafted shoulders at 4 weeks (Figure 4, *A*). Some cartilage-like tissue that stained in safranin O was observed at 4 weeks in the grafted shoulder group.

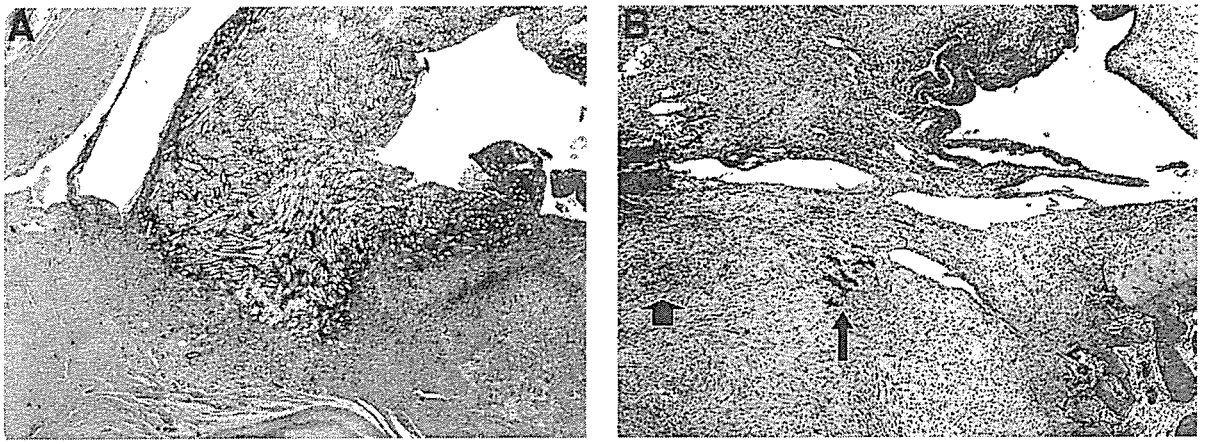

Figure 3 Micrographs from each group 2 weeks after surgery (hematoxylin-eosin stain, original magnification ×40). **A**, Grafted shoulder group. Note that fibroblasts were observed in the fabric at the subacromial bursal side and the tendon-bone insertion. Collagen fibers were not observed. **B**, Control shoulder group. Note the regenerated thin tissue membrane. Blood cells (*short arrow*) and fibrin clot (*long arrow*) were observed at the defect.

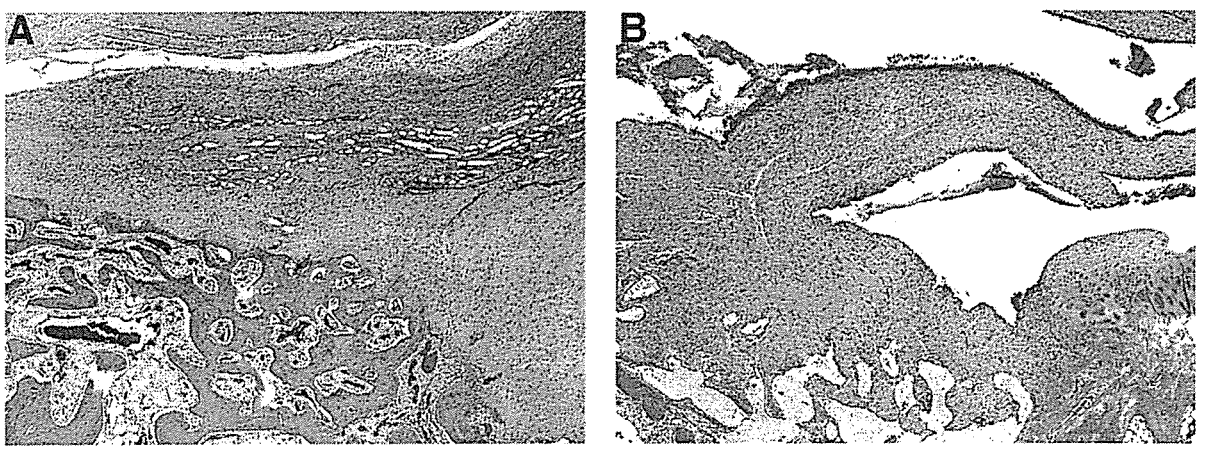

Figure 4 Micrographs from each group 4 weeks after surgery (hematoxylin-eosin stain, original magnification ×40). **A**, Grafted shoulder group. Note that the collagen fibers were well aligned. Trabecular bone was observed at the bony insertion of the chitin. **B**, Control shoulder group. Note that there was a thin membrane with many fibroblasts and vessels.

Microscopically, two pieces of grafted chitin fabric—one at 2 weeks and the other at 4 weeks—were partially detached from the bony trough. On the other hand, in the control shoulder group, the perpendicular pattern of collagen fibers was not found at any time.

Immunohistochemical evaluation

The regenerated tissues in the grafted shoulders were negative for type I collagen, and positive for type III collagen (Figure 7, *A* and *B*). The tendon-bone insertion site was partially positive for type II collagen. However, a normal direct insertion pattern was not found at that site. The immunohistochemical analysis in the control shoulder group was similar to that in the grafted group.

Biomechanical evaluation

Table I summarizes the results of the biomechanical evaluation. In the grafted shoulder group, the failure sites were 4 in the chitin fabric substance and 1 at the tendon-bone junction. In the control shoulder group, 3 specimens failed at midsubstance and 2 failed at the tendon-bone insertion. There was a significant difference in the cross-sectional area between the grafted and control shoulder groups. The failure loads and

Figure 5 Micrograph from grafted shoulder group 8 weeks after surgery (hematoxylin-eosin stain, original magnification ×40). Note that gaps in the chitin fabric had gradually increased, and each fiber was beginning to be absorbed.

stiffness of the grafted shoulder group were significantly greater than those of the control shoulder group.

DISCUSSION

The current surgical procedures for irreparable rotator cuff tears have considerable limitations. To overcome these drawbacks, we focused on applying an acellular matrix to the regeneration of rotator cuff defects. In this study, we hypothesized that chitin fabric could enhance rotator cuff regeneration in the same way that it does in epidermal tissues.

Histologic findings showed that the number of fibroblasts in the grafted shoulder group were significantly greater than those in the control shoulder group. Chitin fabric may play a role in enhancement of cell migration. Previous studies have indicated that chitin accelerated the healing of skin and subcutaneous tissues by increased cell migration.[18,23] Moreover, Okamoto et al[19] reported that chitin implants stimulated abundant angiogenesis. However, in our study, there was no significant difference in angiogenesis between the grafted and control shoulder groups.

In the regeneration of rotator cuff tendons, we must consider not only the number of cells but also the production of extracellular matrix. This study indicated that chitin fabric induced a large amount of collagen fibers. Moreover, we observed that the collagen fibers were in the fabric, and their characteristic crimp patterns were regularly oriented. Although there were a few specimens that detached at the tendon-bone junction, the chitin fabric was able to moderate the mechanical stress, which improved the collagen alignment. Okamoto et al,[19] suggested that chitin supported maturation of collagen fibers. They also suggested that chitin can enhance the production of some cytokines, including interleukin-1 and fibroblast growth factor. The effect on inducing maturation of collagen fibers is associated with the biodegradability of chitin fabric.[19] In our study, the nonwoven chitin fabric had a tendency to be absorbed by 12 weeks after surgery. Sato et al,[22] reported that chitin implants had aggressive tissue ingrowth whereas polylactic acid implant had poor tissue ingrowth in a rabbit Achilles tendon defect model. This result indicated the advantage of chitin fabric as an acellular matrix. The biodegradability of chitin fabric is easily controlled by changing the diameter of the fiber and the density of the fabric. Well-controlled biodegradability of an acellular matrix could provide the space for the maturing extracellular matrix.

Type I collagen is prominent in normal rotator cuff tendon substance, whereas type II collagen is widespread in the insertion zone.[10] Immunohistochemistry showed no difference in the collagen type in the grafted shoulder group compared with the control shoulder group. Although chitin fabric could enhance cell migration and collagen alignment, the fibroblasts produced type III collagen. Several studies have documented that the mechanical properties of healing tissue in tendons and ligaments are inferior to those in native tissue.[1,2,4,5] Frank et al,[5] showed that recovery of the material properties of a ligament scar improved until 14 weeks but the maximum stress or strain remained at a lower level for up to 40 weeks of healing, as compared with a normal ligament. Therefore, this immunohistochemical finding was considered to reveal a limitation in tissue regeneration by use of an acellular matrix. We believe that tissue, including type I collagen, could be regenerated by a tissue engineering technique by using a bioabsorbable scaffold and isolated cells, which is to be addressed in future studies.

The inadequate initial strength of the chitin fabric may cause a recurrent cuff tear or a disability of rotator cuff function in the early healing stage. Histologic findings showed that the regenerated tissue gradually increased until 4 weeks after implantation. In view of the relationship between the recovery time of the regenerated tissue and the absorption rate of chitin fabric, the mechanical strength of chitin fabric 4 weeks after surgery is important for avoiding recurrent tears. We confirmed that the chitin fabric maintained the same failure load after 4 weeks of incubation in culture medium as under dry conditions. However, the stiffness deteriorated during incubation in the culture medium. Sato et al[22] showed that the failure load of chitin and polylactic acid implanted tendons was 39.5% and 53.9% of the value on the intact side, respectively. Future studies should aim at developing novel scaffolds that have a stronger failure load and high stiffness.

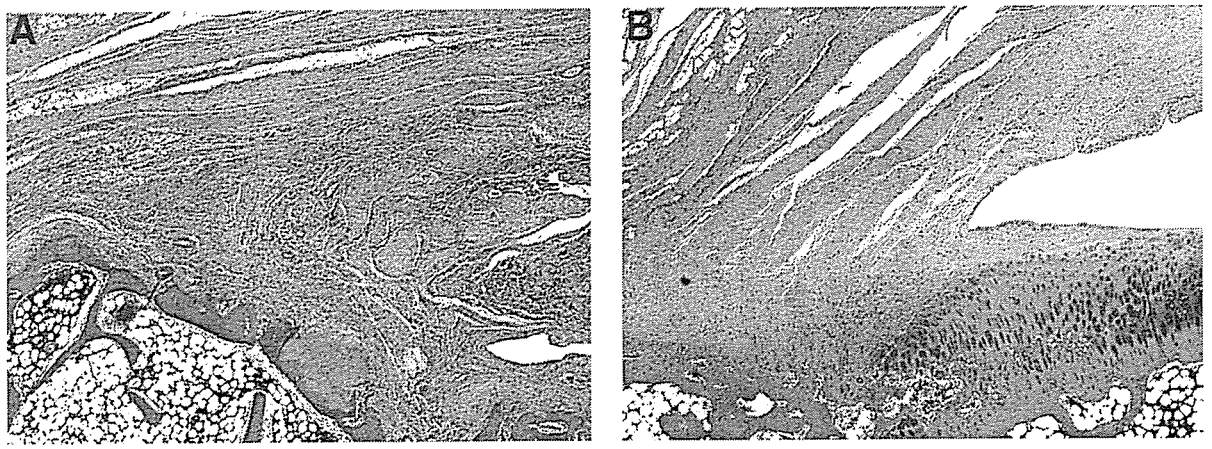

Figure 6 Micrographs from each group 12 weeks after surgery (hematoxylin-eosin stain, original magnification ×40). **A**, Grafted shoulder group. Note that the number of fibroblasts had decreased with the absorption of the fabric. The collagen fibers aggregated in the fabric, and their characteristic crimp patterns were regular and straight. **B**, Control shoulder group. Note that there was thin membrane with less fibroblasts and vessels.

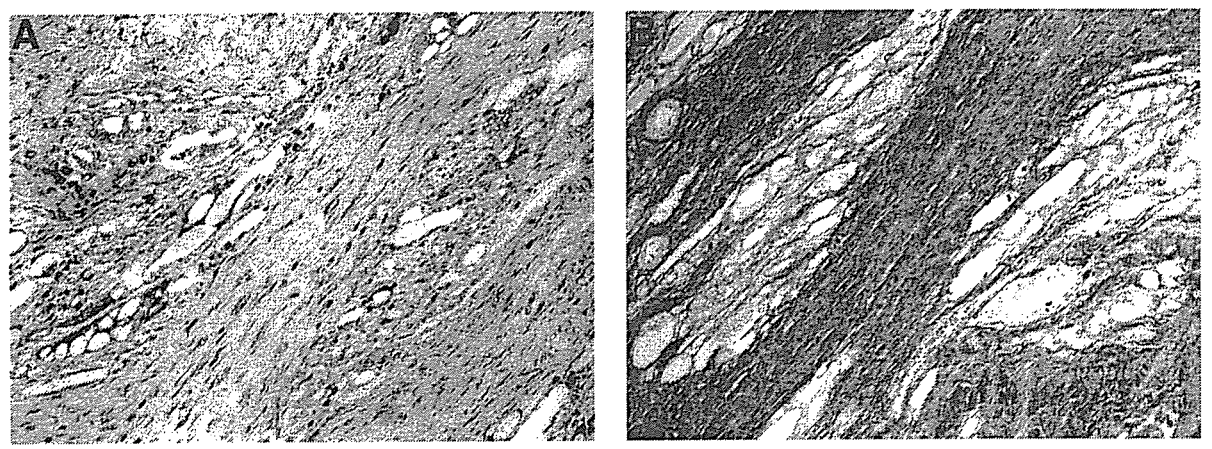

Figure 7 Micrographs of immunostaining in grafted shoulder group 12 weeks after surgery: negative for type I collagen staining (**A**) and positive for type III collagen staining, (**B**) (original magnification ×200).

Table I Mechanical properties of grafted and control shoulder groups

	Cross-sectional area (mm^2)	Failure load (N)	Stiffness (kN/m)
Grafted shoulder group	14.2 ± 5.3*	135.4 ± 28.2*	47.1 ± 13.6*
Control shoulder group	3.7 ± 1.2	12.9 ± 7.1	6.2 ± 2.8

*Significantly different from control shoulder group ($P < .05$) (n = 5).

A further point we must consider is the tendon-bone junction between the humerus and the regenerated tissue. Microscopic findings showed that some materials were detached from the bony trough in the early postoperative period and, in the biomechanical study, that some specimens failed at the tendon-bone insertion. These observations indicate that the method for securing the insertion between the chitin fabric and the bone should be reconsidered.

One of the limitations in our study is that the origin of the cells in the regenerated tissue remained unknown. Moreover, the long-term biodegradability of the chitin in the rotator cuff tendon defect needs clarification. Furthermore, in vivo and in vitro studies

should be conducted to improve the treatment of rotator cuff tendon defects.

In conclusion, using nonwoven chitin fabric as an acellular matrix enhanced cell number and collagen production in a living body. This study provides important and fundamental information for the development of rotator cuff regeneration by use of an acellular matrix. Advanced study is necessary to improve the present material for regeneration of irreparable rotator cuff tears.

We thank Mr Yusuke Matsuda and Mr Ryoichi Tsurutani (Unitica Co, Ltd, Kyoto, Japan) for preparation of the chitin fabric.

REFERENCES

1. Amiel D, Frank CB, Harwood FL, Akeson WH, Kleiner JB. Collagen alteration in medial collateral ligament healing in a rabbit model. Connect Tissue Res 1987;16:357-66.
2. Amiel D, Nagineni CN, Choi SH, Lee J. Intrinsic properties of ACL and MCL cells and their responses to growth factors. Med Sci Sports Exerc 1995;27:844-51.
3. Dejardin LM, Arnoczky SP, Ewers BJ, Haut RC, Clarke RB. Tissue-engineered rotator cuff tendon using porcine small intestine submucosa. Am J Sports Med 2001;29:175-84.
4. Frank C, Schachar N, Dittrich D. Natural history of healing in the repaired medial collateral ligament. J Orthop Res 1983;1:179-88.
5. Frank C, Woo SL, Amiel D, et al. Medial collateral ligament healing: a multidisciplinary assessment in rabbits. Am J Sports Med 1983;11:379-89.
6. Gerber C. Latissimus dorsi transfer for the treatment of irreparable tears of the rotator cuff. Clin Orthop 1992;275:152-60.
7. Hung WS, Fang CL, Su CH, et al. Cytotoxicity and immunogenicity of SACCHACHITIN and its mechanism of action on skin wound healing. J Biomed Mater Res 2001;56:93-100.
8. Hynes RO. Cell adhesion: old and new questions. Trends Cell Biol 1999;9:M33-7.
9. Kimura A, Aoki M, Fukushima S, Ishii S, Yamakoshi K. Reconstruction of a defect of the rotator cuff with polytetrafluoroethylene felt graft: recovery of tensile strength and histocompatibility in an animal model. J Bone Joint Surg Br 2003;85:282-7.
10. Kumagai J, Sarkar K, Uhthoff HK, Okawara Y, Ooshima A. Immunohistochemical distribution of type I, II and III collagens in the rabbit supraspinatus tendon insertion. J Anat 1994;185:279-84.
11. Langer R, Vacanti JP. Tissue engineering. Science 1993;260:920-6.
12. Majima T, Yasuda K, Yamamoto N, Kaneda K, Hayashi K. Deterioration of mechanical properties of the autograft in controlled stress-shielded augmentation procedures: an experimental study with rabbit patellar tendon. Am J Sports Med 1994;22:821-9.
13. Majima T, Yasuda K, Fujii T, et al. Biomechanical effects of stress shielding of the rabbit patellar tendon depend on the degree of stress reduction. J Orthop Res 1996;14:377-83.
14. Malette WG, Quigley HJ, Gaines RD, Johnson ND, Rainer WG. Chitosan: a new hemostatic. Ann Thoracic Surg 1983;36:55-8.
15. Mao J, Zhao L, De Yao K, et al. Study of novel chitosan-gelatin artificial skin in vitro. J Biomed Mater Res 2003;64:301-8.
16. Muzzarelli RA, Mattioli-Belmonte M, Pugnaloni A, Biagini G. Biochemistry, histology and clinical uses of chitins and chitosans in wound healing. EXS 1999;87:251-64.
17. Nerem RM. The challenge of imitating nature. In: Lanza RP, Langer R, Vacanti J, editors. Principles of tissue engineering. 2nd ed. San Diego: Academic Press; 2000. p. 9-15.
18. Okamoto Y, Minami S, Matsuhashi A, et al. Polymeric *N*-acetyl-*D*-glucosamine (chitin) induces histrionic activation in dogs. J Vet Med Sci 1993;55:739-42.
19. Okamoto Y, Southwood L, Stashak TS, et al. Effect of chitin on nonwoven fabric implant in tendon healing. Carbohydr Polym 1997;33:33-8.
20. Ozaki J, Fujimoto S, Masuhara K, Tamai S, Yoshimoto S. Reconstruction of chronic massive rotator cuff tears with synthetic materials. Clin Orthop 1986;202:173-83.
21. Riemersa DJ, Schamhardt HC. The cryo-jaw, a clamp designed for *in vitro* rheology studies of horse digital flexor tendons. J Biomech 1982;15:612-20.
22. Sato M, Maeda M, Kurosawa H, et al. Reconstruction of rabbit Achilles tendon with three bioabsorbable materials: histological and biomechanical studies. J Orthop Sci 2000;5:256-67.
23. Su CH, Sun CS, Juan SW, et al. Development of fungal mycelia as skin substitutes: effects on wound healing and fibroblast. Biomaterials 1999;20:61-8.
24. Thomopoulos S, Soslowsky LJ, Flanagan CL, et al. The effect of fibrin clot on healing rat supraspinatus tendon defects. J Shoulder Elbow Surg 2002;11:239-47.
25. Yusof NL, Lim LY, Khor E. Preparation and characterization of chitin beads as a wound dressing precursor. J Biomed Mater Res 2001;54:59-68.

2-T46 RA肘の屈曲伸展動作解析

中村（なかむら） 順之（よしゆき）[1)]，木村 貞治[2)]，加藤 博之[1)]，斉藤 直人[2)]，村上 成道[1)]，畑 幸彦[1)]

[1)]信州大学整形外科，[2)]信州大学医学部保健学科理学療法学

【目的】関節リウマチ(RA)による肘関節破壊の肘機能障害評価の一法として，表面筋電図，電気角度計，3軸加速度計を用いて，肘屈曲伸展運動時の動態解析を行った．
【対象】関節リウマチ(RA)5名5肘と健常者5名5肘を測定した．
【方法】上腕を下垂位上腕骨回旋中間位で体幹に固定し，前腕回内回外中間位で肘関節最大伸展位から肘関節最大屈曲位までの屈曲伸展運動を0.5Hzで行った．同運動時の上腕二頭筋，上腕三頭筋，腕橈骨筋，橈側手根伸筋，尺側手根伸筋の筋活動を表面筋電計で測定した．さらに同運動時における前腕の3次元加速度を測定した．同時に上肢表面に装着した電気角度計を用いて屈曲時相・伸展時相を評価し，各相における筋電図波形から周波数解析・%MVC・各筋同士の相関を解析した．また加速度波形より周波数を解析した．
【結果】筋電図における肘関節周囲筋群の周波数解析・%MVC・各筋活動の相関はRA群・対照群での明らかな傾向の差は認めなかった．加速度において，肘内外反方向の波形でRA群・健常群でそれぞれ異なる傾向を示し，周波数解析ではRA群でより高い帯域での周波数が計測された．
【考察】肘屈伸運動時の肘内外反方向加速度の解析において，RA群で高い周波数帯域を示した事は，肘関節屈伸運動に際して運動が円滑に行えないことを示唆している．

3-J-EL34

リウマチ上肢の手術治療

加藤 博之[1]　山崎 宏[1]　中村 恒一[1]　岩崎 倫政[2]
三浪 明男[2]

関節リウマチ(RA)による罹患関節の頻度は下肢を含めても手関節，指 MP 関節，肘関節の順に多い．しかし，実際にこれらの上肢関節に手術が行われる頻度は多くはない．その理由は上肢関節における術式とその適応が明確でなく，また手術結果も満足すべきものではなかったことにある．近年 RA 上肢の手術術式は改良され安定した成績が得られてきている．私達の方法と成績を述べる．指ボタン穴変形：PIP 関節の中央索不全と側索の掌側偏位により変形が生じる．PIP の他動伸展がある程度可能な stage II，III 例に Ohshio 変法を行っている．本法は術中に腱緊張度の調節が可能で，後療法が容易である．指 MP 掌尺側偏位：機能障害，疼痛を生じた例ではシリコン性スペーサー治療が一般的である．私達は ball in socket 型人工関節置換術を行っている．本人工関節 99 指の平均 3 年の短期成績を述べる．手関節形成術：尺骨頭の背側脱臼に対してかっては尺骨頭切除術が行われたが，術後の手根骨の尺側偏位や尺骨の切断端の疼痛が問題であった．私達の行っている棚形成術や橈骨月状骨間固定術の適応，方法，成績を述べる．手指伸筋腱皮下断裂：手関節病変に続発して生じるが腱移行，腱移植を組み合わせて治療する．近年は減張位早期運動療法が推奨されている．私達は dynamic splint による早期自動屈曲他動伸展運動を行っている．肘関節形成術：Larsen grade III,IV には津下法による滑膜切除術を行うが，橈骨頭，上腕 3 頭筋腱は温存する．成績は良好である．Larsen grade IV，V には Kudo type 5 人工関節を行っている．最短 2 年(平均 4 年 8 カ月)41 肘の中期成績で再置換を要したのは 1 肘のみであった．臨床成績は全例で改善し術後平均屈曲角度は 134°である．人工肘関節再置換術についても言及する．

[1]信州大整形　[2]北大整形

2-4-200

関節リウマチ指ボタン穴変形に対するOhshio変法の手術手技と成績

Modified Ohshio Procedure for Buttonhole Deformity in Rheumatoid Arthritis

信州大学医学部整形外科
○加藤　博之，山崎　　宏，中村　恒一，
伊坪　敏郎，畑　　幸彦

【目的】関節リウマチ（RA）による指ボタン穴変形に対する治療法は数多いが安定した結果が得られる方法は少ない．私達は外傷性指ボタン穴変形の手術法として報告したohshio法（J．Hand Surg., 15B: 1990）に改良を加え，RA指ボタン穴変形に施行し好結果を得た．

【対象と方法】症例は5例6指で，26～64歳の女性である．内訳は，示指：2指，中指：3指，環指：1指である．ボタン穴変形の程度は，PIP関節の他動完全伸展が可能なstage II：3指，他動的完全伸展が不可能なstage III：3指である．術前の指伸展時のPIP関節屈曲角度は45～60°(平均52°）でDIP関節の過伸展角度は15～30°(平均23°）であった．麻酔はwrist blockとdigital blockを併用した．PIP関節背側に皮切を加え，橈側と尺側の横支靱帯を掌側で切離し，これを背側に翻転した．Stage IIIでは副靱帯と掌側板の切離を行い他動伸展0°を得た．PIP関節の背側で横支靱帯同士を縫合して側索を背側に移動させ，PIP関節の自動伸展0°が得られるように縫合した．次に中節骨背側で側策に対して橈側，尺側から切開を加えDIP関節の自動屈曲30°を得た．術後3日よりDIP関節運動を開始し，術後7日目よりPIP関節運動を開始した．術後期間は最短12カ月である．

【結果と考察】ボタン穴変形は全指で改善した．指伸展時のPIP関節屈曲角度は0～20°(平均8°)，DIP関節伸展角度は0～15°(平均3°）であった．合併症はなく，全例が手術に満足した．本法は術中に指の自動運動を行わせながら腱緊張度を調節できるため，変形の矯正が確実である．また腱の縫合・縫着を要しないので後療法が容易である．

CLOSED RUPTURE OF THE FLEXOR TENDONS OF THE LITTLE FINGER SECONDARY TO NON-UNION OF FRACTURES OF THE HOOK OF THE HAMATE

H. YAMAZAKI, H. KATO, Y. NAKATSUCHI, N. MURAKAMI and Y. HATA

From the Department of Orthopaedic Surgery, Shinshu University School of Medicine, Matsumoto City, Nagano, Japan and the Department of Orthopaedic Surgery, National Nagano Hospital, Ueda City, Nagano, Japan

We report six patients with closed flexor tendon rupture affecting the little finger, occurring secondarily to non-union of the hook of the hamate bone. The ununited fragments were separated from the basal part of the hook by more than 1 mm. The fragments were also rounded and showed marginal sclerosis. Non-union was located in the middle part of the hook in three patients, the tip in two, and the base in one. At operation, the fragments were removed in all patients. Five patients were treated by free tendon grafts using three palmaris and two plantaris grafts and one underwent tendon transfer. Postoperative total range of active motion of the little finger averaged 218° (range 185–265°). All patients returned to their original employment. This series would suggest that flexor tendon rupture can occur after fracture of the hook of the hamate bone, even when the ununited fragment is small and/or rounded.

Journal of Hand Surgery (British and European Volume, 2006) 31B: 3: 337–341

Keywords: hook of hamate, non-union, flexor tendon, closed rupture

INTRODUCTION

Fractures of the hook of the hamate are rare, accounting for less than 2% of all carpal fractures (Andress and Peckar, 1970; Dunn, 1972). Some of these fractures occur in sports while swinging a baseball bat, golf club, or racquet (Bishop and Beckenbaugh, 1988; Stark et al., 1977). Others are caused by falling on the palm, or by a crush injury to the hand (Bishop and Beckenbaugh, 1988). These fractures are often neglected because routine anteroposterior and lateral roentgenograms of the wrist fail to detect them (Murray et al., 1979; Stark et al., 1989) and disability is minimal, or inapparent, in comparison with other fractures of the carpus. In approximately 14% of hamate hook fractures, non-union of the hook may escape discovery until it, eventually, causes closed rupture of the flexor tendons of the little or ring finger (Boulas and Milek, 1990). To date, 26 such cases of tendon rupture have been reported in the English literature (Bishop and Beckenbaugh, 1988; Boyes et al., 1960; Clayton, 1969; Crosby and Linscheid, 1974; Foucher et al., 1985; Futami et al., 1993; Hartford and Murphy, 1996; Milek and Boulas, 1990; Minami et al., 1985; Stark et al., 1977, 1989; Takami et al., 1983; Teissier et al., 1983; Yang et al., 1996), mostly as case reports. Only six reports have described the site of the fracture (Foucher et al., 1985; Hartford and Murphy, 1996; Milek and Boulas, 1990; Minami et al., 1985; Takami et al., 1983; Yang et al., 1996). No reports have described the roentgenographic features of the non-union of the hook of the hamate associated with the tendon rupture.

This study reviews six cases of closed rupture of the flexor tendons of the little finger secondary to non-union of the hook of the hamate, describing characteristic clinical and roentgenographic features of hook non-union causing tendon rupture. The results of tendon reconstruction in these cases are also discussed.

PATIENTS AND METHODS

Between 1990 and 2002, we treated six patients with closed rupture of the flexor tendons of the little finger secondary to non-union of the hook of the hamate (Table 1). The mean age of the patients was 59 (range 35–73) years. All patients were male. Five were manual labourers and the other was an amateur golfer. In four patients, a mild resistance force applied to the little finger precipitated the rupture; in the other two, rupture apparently occurred spontaneously. One of the latter two patients noted gradual progressive inability to flex the little finger; the other noted, one morning, that he could not flex the little finger. At presentation, four of the patients had palmar pain after attempting to flex the little finger. No patient had difficulty flexing the ring finger and no patient had ulnar nerve palsy. The grip strength was recorded in three patients and was an average of 83% of the strength of the contralateral hand (range 71–90%). Three patients had a past episode of trauma to the palm but none had been diagnosed with hamate fracture at the time. Wrist pain had subsided within 3 months of the injury. Three of the four patients whose rupture was precipitated by force had no symptoms referable to the wrist until tendon rupture occurred. The other patient noted mild pain in the palm while playing golf. The period from palmar injury to tendon rupture ranged from 6 months to 25 years. Two

Table 1—Patient data

Patient number	*Age in years*	*Hand/dominance*	*Cause of fracture*	*Type of hamate fracture*	*Time from fracture to tendon rupture*	*Cause of tendon rupture*	*Wrist symptoms before tendon rupture*	*Time from tendon rupture to repair*	*Ruptured tendon(s)/ involved finger*	*Repair*	*Graft length (mm)*	*Follow-up*	*Strickland evaluation*
1	58	Right/dominant	Hammering	Middle part	25 years	Lifting	None	4 weeks	FDP/little	Tendon graft	45	13 years, 6 months	54% (fair)
2	63	Left/nondominant	None apparent	Tip	—	Prying off a cover with a screwdriver	None	9 weeks	FDP + FDS/little	Tendon transfer	—	12 years, 11 months	74% (good)
3	35	Right/dominant	Hit with golf club	Middle part	3 years	Hitting a golf ball	Mild pain on playing golf	8 weeks	FDP/little, frayed FDP/ring	Tendon graft	50	1 year, 2 months	97% (excellent)
4	51	Right/dominant	Impact upon a nail	Base	6 months	Spontaneous	Decrease of grip power	5 weeks	FDP/little	Tendon graft	70	1 year, 11 months	54% (fair)
5	55	Right/dominant	Fall	Middle part	10 years	Lifting	None	6 months	FDP/little, frayed FDS/little	Tendon graft	90	7 years, 3 months	74% (good)
6	73	Left/nondominant	None apparent	Middle part	—	Spontaneous	Occasional pain	7 months	FDP/little	Tendon graft, tenolysis	100	6 years, 3 months	74% (good)

patients, with no recollection of obvious injury to the palm or wrist did heavy manual work as either a woodcutter or a farmer.

Radiographic examination of the wrist included posteroanterior and lateral views in all patients, but none was diagnosed with non-union of the hook of the hamate based upon these radiographs. Radiography in an oblique lateral view in supination was performed in four patients, providing a diagnosis of non-union in two. Radiography in a carpal tunnel view, performed in five patients, was diagnostic in all five; the same was true for computed tomography (CT). Conventional tomography was diagnostic in three of four patients so examined; the same was true for magnetic resonance imaging (MRI). In all patients the fragment had a smooth, round surface at the non-union, associated with marginal sclerosis (Figs 1–3). The fragment varied in size, but, in all instances, it was at least 1 mm away from the body of the hook. The fragment was displaced into the carpal tunnel in one patient (case 2). The hook fractures were located on the middle part of the hook in four patients, on the tip in one and on the base in one patient (Stark et al., 1989).

Tendon reconstruction was performed at an average of 13 weeks after tendon rupture. In all patients, a curved and zigzag incision was made on the palm between the distal palmar crease and the wrist. All patients underwent release of the carpal tunnel for exposure of the hook of the hamate, the tendon stump and the pisotriquetral joint. In all patients, the ruptured tendons were identified at surgery. In four of six patients, only the flexor digitorum profundus (FDP) tendon of the little finger was ruptured and the flexor digitorum superficialis (FDS) tendons were intact. In one patient, the FDP tendon of the little finger was ruptured and the FDS tendon of the ring finger was partially frayed. In the remaining patient, both flexor tendons of the little finger were ruptured. The proximal stumps of the ruptured tendons were in the carpal tunnel and the distal stumps were found proximal to the A1 pulley. No tenosynovitis was apparent around either end of any of the tendons. A free tendon graft, using the palmaris longus tendon in three patients and the plantaris tendon in two, was interposed between the proximal and distal stumps in five patients. Tendon transfer of the FDS tendon of the ring finger, with distal attachment to the FDP tendon of the little finger, was performed in the patient with rupture of both FDP and FDS tendons. In each case, the ends of the ruptured tendon were dissected free of adhesions, and the interpositional graft or tendon transfer tendon was sutured to the freshened stump(s) using the interlacing suture method. The junctions of the grafts with the stumps were placed away from the carpal area. The mean length of the interpositional grafts was 66 (range 45–100) mm. Operative findings included loss of periosteum of the hook of the hamate, which is an important structural component of the ulnar side of the carpal

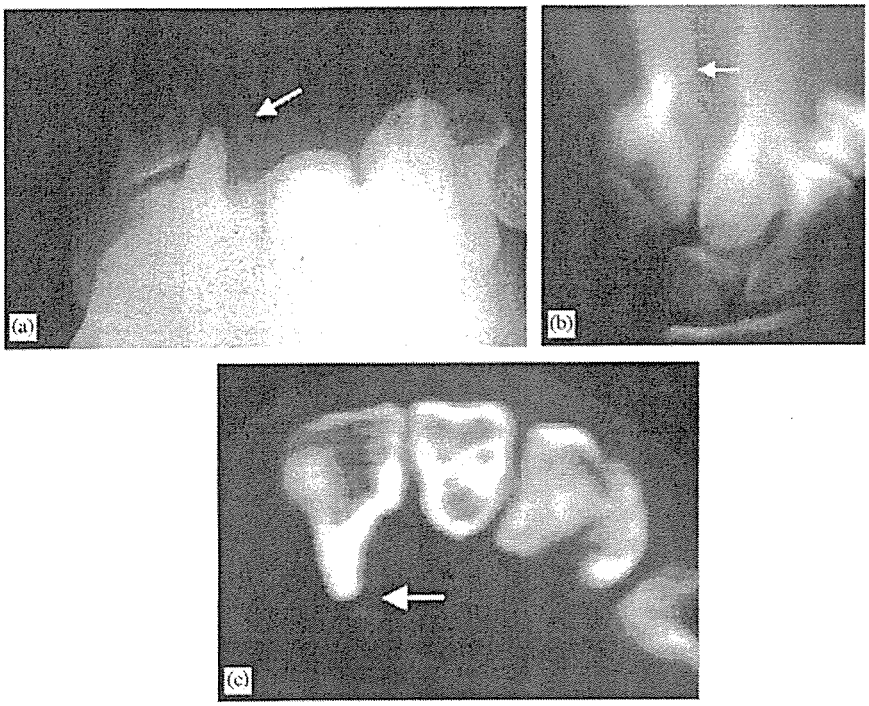

Fig 1 Non-union of the tip of the hook of the hamate bone: (a) on carpal tunnel view X-ray, (b) on tomography, and (c) on CT scan (case 2).

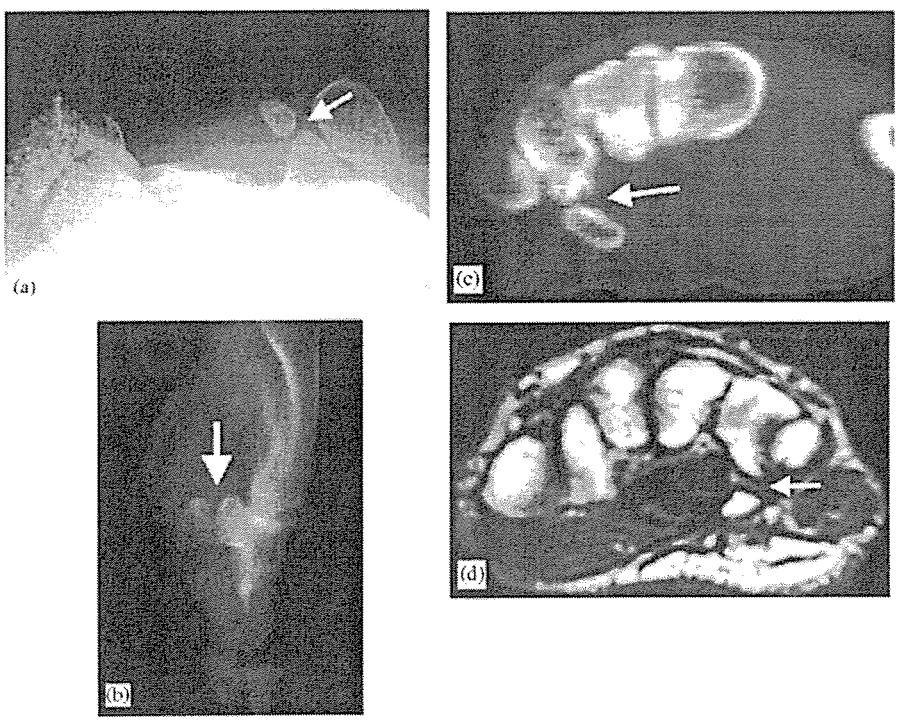

Fig 2 Non-union of the middle part of the hook of the hamate bone: (a) on carpal tunnel view X-ray (case 3), (b) on tomography (case 5), (c) on CT scan (case 1) and (d) on MRI (case 6).

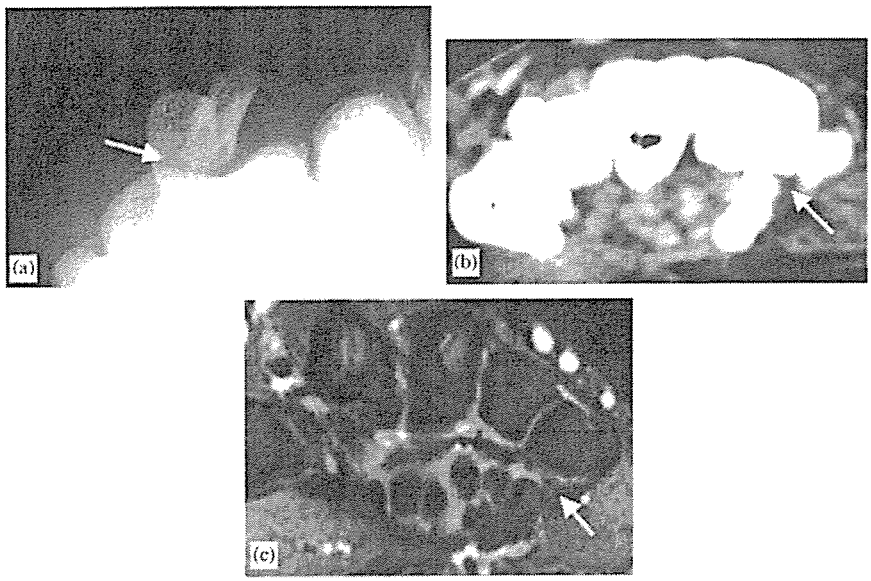

Fig 3 Non-union of the base of the hook of the hamate bone: (a) on carpal tunnel view X-ray, (b) on CT scan and (c) on MRI (case 4).

tunnel. The cortical surface of both the fragment and the basal part of the hook were exposed. The fragments, clearly mobile at the non-union, were removed in all patients. After tendon reconstruction, modified Kleinert mobilization was used for 3–4 weeks. In one patient, tenolysis was performed 14 months after the tendon graft. Follow-up was maintained for an average of 7 years and 2 months (range 1 year and 2 months–13 years and 6 months).

At follow-up, the ranges of active metacarpophalangeal (MCP), proximal interphalangeal (PIP), and distal interphalangeal (DIP) joint motion were measured in all patients and total active range of motion (TAM) was calculated. These findings were also graded according to Strickland's criteria (Strickland and Glogovac, 1980). Grip strength was measured by Smedley's Hand Dynamometer (Sakai Co, Tokyo, Japan) in both hands and grip strength in the affected hand, relative to the contralateral hand, was calculated as a percentage.

RESULTS

Total active range of motion, including MCP, PIP and DIP ranges of motion, averaged 218° (range 185–265°). In full finger extension, the extension deficit at the MCP, PIP and DIP joints averaged 21° (range 5–40°). On average, final grip strength was 86% of the strength of the contralateral hand (range 63–126%). Outcome, as measured by the Strickland's criteria, was excellent in one patient, good in three, and fair in two (Table 2).

All patients were satisfied with the result of tendon reconstruction and all could use the little finger in carrying out activities of daily living, manual labour or sports. All patients returned to their original employment.

DISCUSSION

In all of the patients in our series, symptoms at the wrist from the original fracture had become nil or very mild, until the closed flexor tendon rupture(s) of the little finger occurred. Accordingly, closed flexor tendon injury of the little finger should raise suspicion of non-union of the hook of the hamate. Other causes of tendon injury such as osteoarthritis of the pisotriquetral joint (Saitoh et al., 1997) should be differentiated from non-union of the hook of the hamate by seeking the latter in radiographs from oblique and carpal tunnel views of the wrist, conventional tomography (Murray et al., 1979) or CT (Stark et al., 1989). In three of our patients, MRI was also useful to diagnose non-union of the hook of the hamate.

Stark et al. (1977) reported that 20 of their 62 cases had displaced fragments, fractures having occurred at the base of the hook in 47 cases, in the middle part in eight and at the tip in seven cases. Of 26 cases of closed rupture of the flexor tendon in association with hook of the hamate non-union reported in other papers, the location of the hook fracture was either described, or shown on X-ray, in nine cases, as being at the base in eight cases or in the middle part in one (Foucher et al., 1985; Hartford and Murphy, 1996; Milek and Boulas, 1990; Minami et al., 1985; Takami et al., 1983; Yang et al., 1996). Our cases had fractures at all three sites. The site of non-union appears to have no apparent relationship with the occurrence of flexor tendon rupture.

Murray et al. (1979) pointed out that the ligaments attached to the hook of the hamate transmit intermittent forces that contribute to non-union and irregularity of the fracture margins. From our experience at surgery for painful non-union of the hook of the hamate, the margins of the fragment are sharp and near the basal part of the hook; in contrast, in the present series, the fragments were rounded and fairly distant from the basal portion of the hook, while showing marginal sclerosis at the non-union. This suggests that the tendon abrasion leading to rupture was not caused by a sharp fragment edge at the non-union but by an exposed cortical surface of the non-union that lacked periosteum.

Milek and Boulas (1990) reported surgical results in four patients, three of whom were treated by tendon transfer and one by tendon graft. They attributed variation in quality of the results, largely, to patients' age differences and recommended end-to-side tendon transfer using the FDP tendon of the ring finger. In our series, the mean patient age was 59 years. Although this was relatively high, results were satisfactory and outcome did not depend on patient age or on the interval between tendon rupture and reconstruction. We only had data to show the effectiveness of tendon graft or transfer on grip strength in three patients. To our knowledge, this has not been reported previously. In these three patients (cases 2, 5, and 6) the percentage of the strength of the contralateral hand was 87%, 71%, and 90% pre-operatively and 63%, 79%, and 126% postoperatively. These figures would suggest that tendon reconstruction does not improve grip strength in this situation. This may be because of the presence of an intact FDS tendon in the little finger in five of six of our cases and/or the relatively small contribution of the little finger FDP tendon to entire grip strength, The remaining fully functional fingers of these hands may also have compensated in part for the loss of little finger strength. Use of the FDS tendon of the ring finger as a tendon transfer would seem more likely to compromise not only the function of the ring finger, per se, but also the ability of the hand, as a whole, to compensate for any residual disability of little finger function than restoration of the function of the little finger profundus tendon. Therefore, we believe that free tendon grafting followed by early controlled mobilization is the treatment of first choice for these patients.

References

Andress MR, Peckar VG (1970). Fracture of the hook of the hamate. British Journal of Radiology, 43: 141–143.

Bishop AT, Beckenbaugh RD (1988). Fracture of the hamate hook. Journal of Hand Surgery, 13A: 135–139.

Boulas HJ, Milek MA (1990). Hook of the hamate fractures. Diagnosis, treatment, and complications. Orthopaedic Review, 19: 518–529.

Boyes JH, Wilson JN, Smith JW (1960). Flexor-tendon ruptures in the forearm and hand. American Journal of Orthopedics, 42: 637–646.

Clayton Ml (1969). Rupture of the flexor tendons in the the carpal tunnel (non-rheumatoid) with specific reference to fracture of the hook of the hamate. Journal of Bone and Joint Surgery, 51A: 798–799.

Crosby EB, Linscheid RI (1974). Rupture of the flexor profundus tendon of the ring finger secondary to a fracture of the hook of the hamate. Review of the literature and report of two cases. Journal of Bone and Joint Surgery, 56A: 1076–1078.

Dunn AW (1972). Fractures and dislocations of the carpus. Surgical Clinics of North America, 52: 1513–1538.

Foucher G, Schuind F, Merle M, Brunelli F (1985). Fractures of the hook of the hamate. Journal of Hand Surgery, 10B: 205–210.

Futami T, Aoki H, Tsukamoto Y (1993). Fractures of the hook of the hamate in athletes. 8 cases followed for 6 years. Acta Orthopaedica Scandinavica, 64: 469–471.

Hartford JM, Murphy JM (1996). Flexor digitorum profundus rupture of the small finger secondary to nonunion of the hook of hamate: a case report. Journal of Hand Surgery, 21A: 621–623.

Milek MA, Boulas HJ (1990). Flexor tendon ruptures secondary to hamate hook fractures. Journal of Hand Surgery, 15A: 740–744.

Minami A, Ogino T, Usui M, Ishii S (1985). Finger tendon rupture secondary to fracture of the hamate. A case report. Acta Orthopaedica Scandinavica, 56: 96–97.

Murray WT, Meuller PR, Rosenthal DI, Jauernek RR (1979). Fracture of the hook of the hamate. American Journal of Roentgenology, 133: 899–903.

Saitoh S, Kitagawa E, Hosaka M (1997). Rupture of flexor tendons due to pisotriquetral osteoarthritis. Archives of Orthopaedic and Trauma Surgery, 116: 303–306.

Stark HH, Chao EK, Zemel NP, Rickard TA, Ashworth CR (1989). Fracture of the hook of the hamate. Journal of Bone and Joint Surgery, 71A: 1202–1207.

Stark HH, Jobe FW, Boyes JH, Ashworth CR (1977). Fracture of the hook of the hamate in athletes. Journal of Bone and Joint Surgery, 59A: 575–582.

Strickland JW, Glogovac SV (1980). Digital function following flexor tendon repair in zone II: a comparison of immobilization and controlled passive motion techniques. Journal of Hand Surgery, 5A: 537–543.

Takami H, Takahashi S, Ando M (1983). Rupture of flexor tendon associated with previous fracture of the hook of the hamate. Hand, 15: 73–76.

Teissier J, Escare P, Asencio G, Gomis R, Allieu Y (1983). Rupture of the flexor tendons of the little finger in fractures of the hook of the hamate bone. Report of two cases. Annales de Chirurgie de la Main, 2: 319–327.

Yang SS, Kalainov DM, Weiland AJ (1996). Fracture of the hook of hamate with rupture of the flexor tendons of the small finger in a rheumatoid patient: a case report. Journal of Hand Surgery, 21A: 916–917.

Received: 24 July 2005
Accepted after revision: 30 December 2005
Dr Hiroshi Yamazaki, MD, Department of Orthopaedic Surgery, Shinshu University School of Medicine, 3-1-1, Asahi, Matsumoto City, Nagano, 390-0304, Japan. Tel.: +81 263 37 2659; fax: +81 263 35 8844.
E-mail: h-ymzk@hsp.md.shinshu-u.ac.jp

doi:10.1016/j.jhsb.2005.12.015 available online at http://www.sciencedirect.com

Eur Spine J
DOI 10.1007/s00586-006-0234-5

ORIGINAL ARTICLE

Computer-assisted screw insertion for cervical disorders in rheumatoid arthritis

Jun Takahashi · Yasuhiro Shono · Isao Nakamura · Hiroki Hirabayashi · Mikio Kamimura · Sohei Ebara · Hiroyuki Kato

Received: 23 January 2006 / Revised: 4 September 2006 / Accepted: 12 September 2006

Abstract To reconstruct highly destructed unstable rheumatoid arthritis (RA) cervical lesions, the authors have been using C1/2 transarticular and cervical pedicle screw fixations. Pedicle screw fixation and C1/2 transarticular screw fixation are biomechanically superior to other fixation techniques for RA patients. However, due to severe spinal deformity and small anatomical size of the vertebra, including the lateral mass and pedicle, in the most RA cervical lesions, these screw fixation procedures are technically demanding and pose the potential risk of neurovascular injuries. The purpose of this study was to evaluate the accuracy and safety of cervical pedicle screw insertion to the deformed, fragile, and small RA spine lesions using computer-assisted image-guidance systems. A frameless, stereotactic image-guidance system that is CT-based, and optoelectronic was used for correct screw placement. A total of 21 patients (16 females, 5 males) with cervical disorders due to RA were surgically treated using the image-guidance system. Postoperative computerized tomography and plane X-ray was used to determine the accuracy of the screw placement. Neural and vascular complications associated with screw insertion and postoperative neural recovery were evaluated. Postoperative radiological evaluations revealed that only 1 (2.1%; C4) of 48 screws inserted into the cervical pedicle had perforated the vertebral artery canal more than 25% (critical breach). However, no neurovascular complications were observed. According to Ranawat's classification, 9 patients remained the same, and 12 patients showed improvement. Instrumentation failure, loss of reduction, or nonunion was not observed at the final follow-up (average 49.5 months; range 24–96 months). In this study, the authors demonstrated that image-guidance systems could be applied safely to the cervical lesions caused by RA. Image-guidance systems are useful tools in preoperative planning and in transarticular or transpedicular screw placement in the cervical spine of RA patients.

Keywords Cervical spine · Image guidance · Rheumatoid arthritis · Cervical pedicle screw · Transarticular screw

J. Takahashi (✉) · I. Nakamura · H. Hirabayashi · H. Kato
Department of Orthopaedic Surgery,
Shinshu University, School of Medicine,
Matsumotoshi Asahi 3-1-1,
Nagano 390-8621, Japan
e-mail: jtaka@hsp.md.shinshu-u.ac.jp

Y. Shono
Department of Orthopaedic Surgery,
Hokkaido Social Insurance Hospital,
Sapporoshi Toyohiraku Nakanoshima Ichijyo, 8-3-18,
Hokkaido 062-8618, Japan

M. Kamimura
Kamimura Clinic, Matsumotoshi Kotobuki Toyooka
Ipponmatsu 595-17, Nagano 399-0021, Japan

S. Ebara
Department of Orthopaedic Surgery,
Chigasaki Tokushukai Medical Center,
Chigasakishi Saiwaityo 14-1,
Kanagawa 253-0052, Japan

Introduction

There are various cervical disorders caused by rheumatoid arthritis (RA). The most common disorders

include atrantoaxial (C1/2) instability and subluxation in the mid- and lower-cervical spine [6, 21]. These conditions sometimes cause myelopathy, severe pain, or both, either of which impairs the quality of life of RA patients [19]. In such cases, reconstruction surgery may be indicated. Posterior procedures using sublaminar wiring or hook systems have been employed; however, these sometimes result in loss of reduction and/or nonunion [20, 24]. Innovative methods such as C1/2 transarticular and cervical pedicle screw techniques provide greater biomechanical stability compared to conventional posterior fusion techniques [9, 14]. Jones et al. [10] reported that cervical pedicle screws have a significantly higher resistance to pull-out forces than lateral mass screws. However, due to severe spinal deformity and small anatomical size of the vertebra including the lateral mass and pedicle in most of the RA cervical lesions, these screw fixation procedures are technically demanding and pose the potential risk of neurovascular injuries [7, 16, 27]. Frameless stereotactic technology was first designed for intra-cranial surgery for guidance of unseen lesions [8]. Computer-assisted techniques were introduced in spine surgery in the 1990s to improve accuracy and safety of operative procedures [3, 18]. CT-based optoelectronic navigation was originally introduced by Nolte et al. [18]. Amiot et al. [3] later performed this technique in vitro with a magnetic-field based navigator, however this never really gained clinical acceptance. Laine et al. [15] presented evidence for improvement of accuracy under clinical conditions using this technique. In 1996, we started the laboratory testing the clinical application of computer-assisted spine surgery [11, 12]. To improve the accuracy of screw placement, we have adopted an image-guidance system and herein report the usefulness and the limitations of this technique, in the area of surgical reconstruction of RA cervical spine lesions.

Materials and methods

Between January 1998 and January 2004, a total of 21 patients (16 females, 5 males) with cervical disorders due to RA were surgically treated using the image-guidance system. The mean age at the time of surgery was 60.8 years (range 51–78 years). Twelve of the 21 patients displayed typical mutilating-type joint involvements with severe cervical lesion. The cervical disorders were atlanto-axial subluxation (AAS) in six cases, AAS and vertical subluxation of the atlas (VS) in three, subaxial subluxation (SAS) in four and AAS + VS + SAS in eight. According to Ranawat's classification [19], the neurological deficits were class 2 in five cases, class 3A in seven, and class 3B in nine. The Ranawat's classification is defined as follows; class 1, no neural deficit; class 2, subjective weakness with hyper-reflexia and dysesthesia; class 3A, objective findings of paresis and long-tract signs, but ambulation possible; class 3B, quadriparesis with resultant inability to walk or to feed oneself.

Occipital or cervical pain was classified into four grades according to Ranawat's criteria [19]: Grade 0, None; Grade 1, mild, intermittent, requiring only aspirin analgesia; Grade 2, moderate, cervical collar required; Grade 3, severe, pain not relieved by either aspirin or collar. Preoperative pain assessments were Grade 0 in one case, Grade 1 in seven cases, Grade 2 in eleven cases, and Grade 3 in two cases.

Preoperative MR angiography was performed in all patients to evaluate conditions of the bilateral vertebral artery. Patients with 50% stenosis or more were classified as stenosis patients, while those with invisible vertebral artery were classified as occlusion patients. In case of vertebral artery occlusion or stenosis, no pedicle screws were used in the artery-dominant side to avoid vertebrobasilar ischaemia and concurrent stroke if pedicle diameter was narrow.

A frameless stereotactic image-guidance system (Stealth Station and Stealth Station TREON^{TM}; Medtronic, Sofamor Danek, Memphis, TN, USA) was used for correct screw placement and fixation of the cervical spine. The basic data used for navigation were preoperative CT scan imaging data, consisting of consecutive axial slices, 1 mm in thickness of the cervical spine of the RA patients. The data were transferred to the system computer and were reconstructed into two-dimensional (2-D) and three-dimensional (3-D) images on a video monitor. Other mechanical components consisted of a computer workstation, a surgical reference frame, a probe rod to indicate the position in the surgical field, infrared light-emitting diodes (LEDs) that were attached to the probe rod, an electro-optical camera as a position sensor connected to the computer, and a drill guide. Infrared beams were tracked by the electro-optical camera system and the position of the respective LEDs was identified in real time in the surgical field.

Registration was performed in order to accurately match the computer-reconstructed 3-D surgical space with the real surgical space, by identifying four or more points on the vertebrae and the corresponding points of the vertebrae on the 3-D CT image on the monitor (matched-pair point registration). Though more precise matching of the two spaces is usually obtained by repeated registration procedures with 30 or more

randomized points indicated by the probe on the surface of the vertebral body (surface registration), this group's procedure employs only five to six registration points for two consecutive lamina, to shorten the surgical time. More accurate positioning is possible by using the top of the spinous process and bilateral inferior facet caudal tip as points.

We established a surgical plan a day before surgery and confirmed insertion point of screws, applicability of 3.5 mm screws, point-for-point registration, plus in Magerl's screw procedure, screw position in relation to vertebral artery. This planning procedure took 20–40 min. Evaluation during the surgical plan for navigation provides further benefit by identifying pedicles with insertion risks and excluding such pedicles from operation (about 10% of all pedicles were excluded). Then, the entrance holes, direction, diameter, and depth of the screws were depicted with a cursor on the monitor, and the surgery was initiated. After exposure of the posterior bony elements of the spine, the reference frame was fixed to the spinous processes and the registration procedures described above were performed. After completion of the registration by matched-pair point and surface registration, the screws were inserted under the guidance of the navigation system. The position of the probe or drill guide was superimposed in real-time on CT images on the monitor, and the screws were introduced into the pedicles at the planned position indicated on the monitor (Fig. 1). The required time between fixation of reference frame to spinous process and insertion of pedicle screw to each segment (1 or 2 vertebrae) was 10–15 min. After all screws were set, the reference frame for registration was removed and additional surgical procedures including decompression or bone graft were followed. If pedicle screw insertion was ineligible, sublaminar cable fixation by SecureStrand was performed.

The following surgical procedures were performed with the aid of image-guidance systems: C1/2

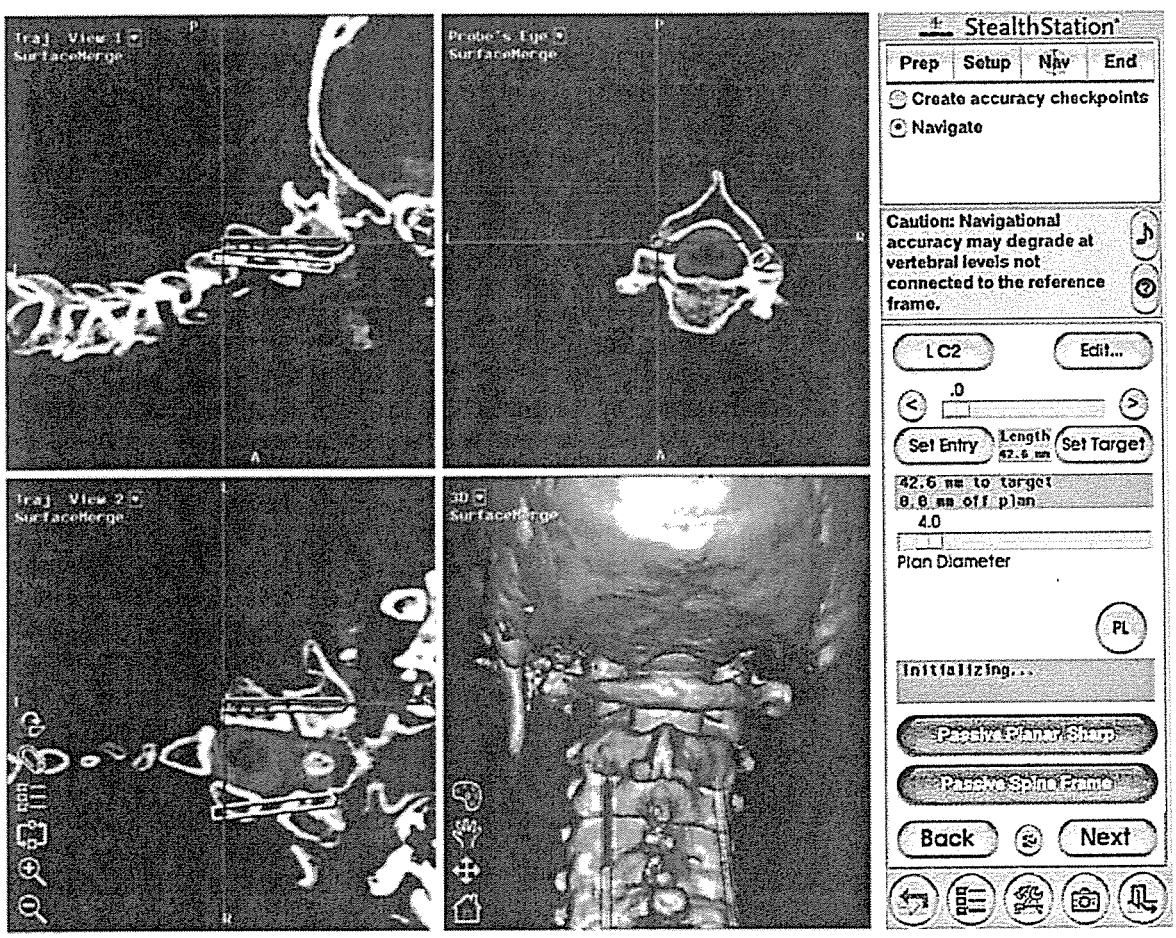

Fig. 1 Computer display shown at surgery. The position of the device and surgical plan are shown in four views. The *narrow gray arrow* indicates the position and direction of the device, and the *wide white arrow* indicates the planned screw trajectory

transarticular screw (Trans Bone Screw; KiscoMedica, St Priest, France) fixation (Magerl's procedure [17]) in six patients, cervicothoracic fusion using transpedicular screws (Cervical Pedicle Screw System; Depuy Spine, Inc., Raynham, MA) in four patients, occipitocervical or occipitothoracic fusion using the Olerud cervical system (Nord Opedic, Askim, Sweden) in six patients, and RRS Loop Spinal System (Robert Leid, Tokyo, Japan) in five patients (Table 1). All patients had autogenous iliac bone grafts. Patients were permitted to stand and walk from the day after the operation without a collar, since pedicle screw fixation provided enough stability to ambulate without it. Radiological assessment of screw placement was performed using Kast's criteria [13]. All patients underwent reconstruction CT scans with plain a.p., lateral and oblique X-ray films of instrumented levels after surgery.

Clinical results were based on invitations of patients to follow-up. The surgeon performed the follow-up investigation and performed radiographic assessment.

Results

A total of 81 screws, including twelve C1/2 transarticular screws and 69 transpedicular screws (C2; 11 screws, C3; 5, C4; 6, C5; 3, C6; 7, C7; 16, T1; 17, T2; 4), were inserted using image-guidance system. Based on Kast's criteria [13], correct placement of the 12 transarticular screws and 69 transpedicular screws (48 cervical pedicle screws and 21 thoracic pedicle screws) was assessed.

Correct screw position

Screws either completely within cortical walls of the pedicle or with a maximal cortical perforation of 1 mm as seen on CT. This group comprised 75 (93%) of implanted screws, including transarticular and thoracic pedicle screws.

Minor breach

Lateral or ventral perforation of the vertebral body (2 screws; T1, T2), slight affection of the lateral recess without dural contact (1 screw: C5) or narrowing of the vertebral artery canal less than 25% of its diameter (2 screws; C4, C6). In summary, 5 screws (6% of all screws) showed a minor breach radiologically.

Major breach

Encroachment of the vertebral artery canal of more than 25% (1 screw: C4, case 6) or caudal perforation of

Table 1 Clinical profile and details of surgical procedures

Case	Age at surgery (years)	Gender	Follow-up (months)	Cervical disorder	Surgical procedure	Extent of fusion	Laminectomy or Laminoplasty	Device
1	54	M	96	AAS	Magerl & Brooks	C1-2	C3-7	TBS
2	56	F	89	AAS + VS + SAS	O-T fusion	C0-T2	C1,C3-5	Olerud
3	63	F	74	AAS + VS + SAS	O-T fusion	C0-T1	N	Olerud
4	63	F	72	AAS + VS + SAS	O-T fusion	C0-T1	C1,C3-6	Olerud
5	62	F	70	AAS + VS + SAS	O-T fusion	C0-T1	C1	Olerud
6	72	M	66	AAS + VS + SAS	O-T fusion	C0-T1	C1,C3-7	Olerud
7	62	M	58	AAS + VS + SAS	O-C fusion	C0-7	C1	Olerud
8	76	F	51	SAS	C-T fusion	C4-T1	C5-6	CPSS
9	54	M	50	AAS	Magerl & Brooks	C1-2	N	TBS
10	62	F	48	AAS + VS	O-C fusion	C0-5	C1	RRS
11	58	F	45	SAS	C-T fusion	C6-T2	C7-T1	CPSS
12	78	F	42	AAS + VS + SAS	O-T fusion	C0-T1	C1	RRS
13	67	F	40	AAS	Magerl & Brooks	C1-2	N	TBS
14	54	F	39	AAS + VS	O-C fusion	C0-2	C1	RRS
15	63	F	36	AAS + VS	O-C fusion	C0-2	C1	RRS
16	53	M	32	AAS + VS + SAS	O-C fusion	C0-7	C1, C3-6	RRS
17	54	F	29	SAS	C-T fusion	C5-T1	C6	CPSS
18	67	F	27	AAS	Magerl & Brooks	C1-2	C3-6	TBS
19	51	F	27	AAS	Magerl & Brooks	C1-2	N	TBS
20	57	F	25	SAS	C fusion	C3-4	C3-6	CPSS
21	51	F	24	AAS	Magerl & Brooks	C1-2	N	TBS

AAS atlanto-axial subluxation, *VS* vertical subluxation, *SAS* subaxial subluxation,

O-C occipitocervical, *O-T* occipitothoracic, *C* cervical, *N* no

TBS trans bone screw, *CPSS* cervical pedicle screw system, *RRS* RRS loop spinal system

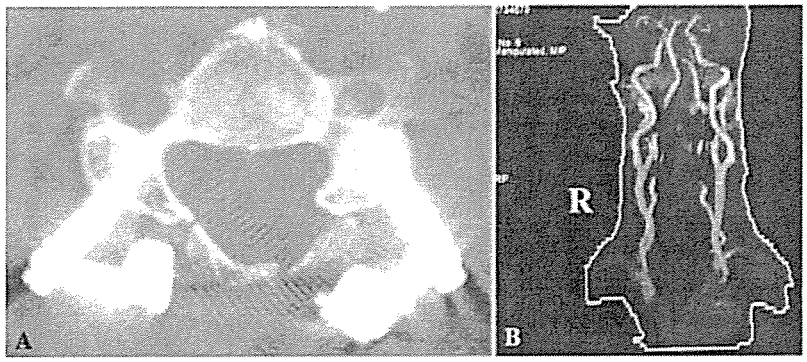

Fig. 2 **a** Patient (case 6) with screw displacement C4 with narrowing of the vertebral channel more than 25% (left screw); major breach. **b** Postoperative MR angiography revealed no vertebral artery occlusion

the pedicle with potential nerve root compression or injury (0 screws) were observed. Further, major breaches like medial pedicle perforation with dural laceration and risk of radicular or medullar compression or injury were not observed in this series. The group of major breaches comprised only one (1.2%) of implanted screws (81 screws) or one (2.1%) of all implanted cervical pedicle screws (48 screws), without injury to the vertebral artery. Although the authors had confirmed no pedicle wall perforation during the probing procedure, CT evaluation showed lateral pedicle wall perforation (major breach) in one screw (C4 pedicle screw) (Fig. 2). This perforation may have been caused during reduction and/or screw-rod connecting maneuvers in which unexpected excessive load had acted on the screw. Postoperative MR angiography revealed no vertebral artery occlusion (Fig. 2).

Preoperative vertebral artery evaluation by MR angiography showed four (19%; three cases with AAS + VS + SAS and one case with AAS + VS) unilateral stenosis and one (4.8%; AAS + VS + SAS) unilateral occlusion. Average operative time was 275 min (range 148–505 min) and the average intraoperative blood loss was 380 ml (range 20–630 ml). According to Ranawat's classification, 9 patients remained the same (2 → 2; 4 patients, 3A → 3A; 3, 3B → 3B; 2) and 12 patients showed improvement (2 → 1; 1 patient, 3A → 2; 4, 3B → 3A; 7) (Table 2). Seven of the 9 patients who could not walk (3B) before surgery could walk (3A) post surgery. All patients maintained the improved ADL level throughout the postoperative course. In 18 of the 21 cases (86%), occipital or neck pain as classified by Ranawat's criteria for pain had improved.

No instrumentation failure, loss of reduction, or nonunion had occurred at the final follow-up (average 49.5 months; range 24–96 months). Bony fusion was defined as an absence of segmental motion in functional lateral X-rays with presence of solid bony union observed in reconstruction CT (Fig. 3, case 5). Solid union was achieved in all 21 patients.

Table 2 The neurological deficit class before surgery and at the final assessment

Preoperative neurological deficit class	Follow-up neurological deficit class			
	3B	3A	2	1
3B	2	7		
3A		3	4	
2			4	1

Case presentations

Two typical cases with extremely narrow pedicles are shown. With conventional transarticular or transpedicle screw insertion techniques, iatrogenic neurovascular injuries due to malposition of the screws may have resulted.

Case 9

This patient was a 54-year-old man with AAS. Transarticular screw fixation (Trans Bone Screw; Kisco-Medica, France) was inserted using the navigation system and image intensifier, lateral view. Posterior bone graft was performed with Brooks' method using SecureStrand sublaminar cables (Pioneer Surgical Technology, Marquette, MI) (Fig. 4). After 50 months post-surgery, the patient showed improvement from 2 (preoperatively) to 1 according to Ranawat's classification, and occipital pain was reduced (2 → 1) (Fig. 5).

Case 10

This patient was a 62-year-old woman with non-reducible AAS and VS. In preoperative planning, the